



## Trophic regions of a hydrothermal plume dispersing away from an ultramafic-hosted vent-system: Von Damm vent-site, Mid-Cayman Rise

**Sarah A. Bennett**

*NASA Jet Propulsion Laboratory, California Institute of Technology, 4800 Oak Grove Drive, Pasadena, California, 91109, USA (sarah.a.bennett@jpl.nasa.gov)*

**Max Coleman**

*NASA Jet Propulsion Laboratory, California Institute of Technology, Pasadena, California, USA*

*NASA Astrobiology Institute, Pasadena, California, USA*

**Julie A. Huber and Emily Reddington**

*Josephine Bay Paul Center, Marine Biological Laboratory, Woods Hole, Massachusetts, USA*

**James C. Kinsey, Cameron McIntyre, Jeffrey S. Seewald, and Christopher R. German**

*Woods Hole Oceanographic Institution, Woods Hole, Massachusetts, USA*

[1] Deep-sea ultramafic-hosted vent systems have the potential to provide large amounts of metabolic energy to both autotrophic and heterotrophic microorganisms in their dispersing hydrothermal plumes. Such vent-systems release large quantities of hydrogen and methane to the water column, both of which can be exploited by autotrophic microorganisms. Carbon cycling in these hydrothermal plumes may, therefore, have an important influence on open-ocean biogeochemistry. In this study, we investigated an ultramafic-hosted system on the Mid-Cayman Rise, emitting metal-poor and hydrogen sulfide-, methane-, and hydrogen-rich hydrothermal fluids. Total organic carbon concentrations in the plume ranged between 42.1 and 51.1  $\mu\text{M}$  (background =  $43.2 \pm 0.7 \mu\text{M}$  ( $n=5$ )) and near-field plume samples with elevated methane concentrations imply the presence of chemoautotrophic primary production and in particular methanotrophy. In parts of the plume characterized by persistent potential temperature anomalies but lacking elevated methane concentrations, we found elevated organic carbon concentrations of up to 51.1  $\mu\text{M}$ , most likely resulting from the presence of heterotrophic communities, their extracellular products and vent larvae. Elevated carbon concentrations up to 47.4  $\mu\text{M}$  were detected even in far-field plume samples. Within the Von Damm hydrothermal plume, we have used our data to hypothesize a microbial food web in which chemoautotrophy supports a heterotrophic community of microorganisms. Such an active microbial food web would provide a source of labile organic carbon to the deep ocean that should be considered in any future studies evaluating sources and sinks of carbon from hydrothermal venting to the deep ocean.

**Components:** 6,500 words, 5 figures, 2 tables.

**Keywords:** hydrothermal; food web; microorganisms; plume; carbon; ultramafic.

**Index Terms:** 4817 Food webs and trophodynamics: Food webs, structure, and dynamics (0491); 0330 Geochemical cycles: Geochemical cycles (1030).

Received 20 July 2012; Revised 2 January 2013; Accepted 7 January 2013; Published 22 February 2013.

Bennett, S. A., M. Coleman, J. A. Huber, E. Reddington, J. C. Kinsey, C. McIntyre, J. S. Seewald, and C. R. German (2013), Trophic regions of a hydrothermal plume dispersing away from an ultramafic-hosted vent-system: Von Damm vent-site, Mid-Cayman Rise, *Geochem. Geophys. Geosyst.*, 14, 317–327, doi:10.1002/ggge.20063.

## 1. Introduction

[2] Ridge-crest hydrothermal systems represent a biological habitat in the deep ocean that exist both on a local scale (vent fauna) [Corliss *et al.*, 1979; Van Dover, 2000] and in the overlying water column (plume microorganisms) [Winn *et al.*, 1986]. Hydrothermal vents emit chemically-reduced fluids into the open ocean, which are diluted with surrounding seawater. The disequilibria set up between the reduced chemicals exiting the seafloor and the more oxidizing species present in ocean water provides the energy required for chemosynthesis: the biological conversion of inorganic carbon and methane to more complex organic molecules using chemical energy instead of sunlight.

[3] At high-temperature vents ( $>100^{\circ}\text{C}$ ), the emitted fluids are so much less dense than the surrounding seawater that they rise up into the water column in a turbulent buoyant plume that experiences an approximately  $10^4$ -fold dilution with the surrounding seawater. By the time the plume becomes nonbuoyant, a few hundred meters off the seafloor, it disperses away from the vent site due to local currents [Lupton *et al.*, 1985; German and Seyfried, In press]. Owing to kinetic barriers that preclude rapid oxidation, the concentrations of reduced species in the nonbuoyant plume remain elevated compared to the open ocean, creating the potential for plume-hosted microbial activity some distance from the hydrothermal vent source [Winn *et al.*, 1986; Lesniewski *et al.*, 2012; Sylvan *et al.*, 2012]. Significant metabolic energy can be gained from the oxidation of hydrogen, methane, and metal sulfides in hydrothermal plumes, as long as abiotic oxidation reactions are kinetically inhibited [McCollom, 2000].

[4] High-temperature venting associated with serpentinization of ultramafic rocks is characterized by high hydrogen and methane concentrations in end-member fluids released at the seafloor (e.g., Rainbow; Charlou *et al.* [1998]). These systems have the potential to provide a larger amount of metabolic energy to the microbial community per liter of hydrothermal fluid compared to basalt-hosted

systems where hydrogen and methane concentrations are generally lower. Ultramafic systems also have the potential to host abiotic organic carbon synthesis deep within the crust through Fischer-Tropsch type synthesis [Shock, 1990; Shock and Schulte, 1998] and may provide a further energy source to heterotrophic microorganisms.

[5] In this study, we have sampled the ultramafic-influenced Von Damm hydrothermal system on the Mid-Cayman Rise (MCR) first reported by Connelly *et al.* [2012]. The site comprises a 200 m diameter mound located on the eastern slope of an oceanic core complex (Mt Dent) located 13 km west of the axial rift-valley of the MCR at this latitude [Hayman *et al.*, 2011]. This system lacks typical “black smokers” associated with many high-temperature vent fields and instead hosts hot, clear fluids that emanate from the summit of the mound, yielding a buoyant plume rich in methane and hydrogen sulfide, but low in metals [Connelly *et al.*, 2012].

## 2. Methods

### 2.1. Plume Detection

[6] In August 2011, the Von Damm hydrothermal plume was sampled systematically as part of a telepresence-enabled Ocean Exploration cruise aboard the NOAA ship *Okeanos Explorer* [German *et al.*, 2012a, 2012b]. Plume investigations were carried out using a SeaBird 9/11+ conductivity-temperature-depth (CTD)-rosette equipped with a light scattering sensor (LSS), an oxidation-reduction potential sensor, and a dissolved oxygen sensor. The rosette was also equipped with an ultrashort baseline navigation beacon, which allowed for processed water column data to be merged with the exact position of the CTD at depth. Data processing was carried out at the NASA Jet Propulsion Laboratory and Woods Hole Oceanographic Institution immediately following each CTD-rosette recovery to provide the three scientists on board the ship, together with the shore-based science party, with a three-dimensional image of the plume merged with underlying bathymetry to aid decisions for further deployments. A total of three

Tow-Yo operations (CTD 2, 3 and 4) and one vertical cast (CTD 7) were carried out within the dispersing Von Damm hydrothermal plume (Figure 1).

[7] This cruise also involved a remotely operated vehicle component that was limited to video reconnaissance of the Von Damm mound and surrounding areas. A subsequent cruise in January 2012 to the MCR, quantified the temperature of the Von Damm end-member fluids using a high-temperature probe operated by the remotely operated vehicle Jason [German *et al.*, 2012b]. Further data on the vent fluid composition collected during this cruise will be reported elsewhere.

## 2.2. Sample Collection, Processing, and Analysis

[8] A suite of water column samples was collected by CTD rosette from the dispersing hydrothermal plume using 2.5 L bottles. Water samples were collected based on real-time feedback from the CTD and in particular, the in situ LSS and oxidation-reduction potential sensors. On recovery of the CTD rosette aboard ship, water samples were collected for shipboard methane (CH<sub>4</sub>) analysis, and shore-based total organic carbon (TOC) and cell count analyses.

### 2.2.1. Methane Analysis

[9] Water samples for methane analysis (20 mL) were drawn from the Niskin bottles in 60 mL plastic

syringes. Dissolved CH<sub>4</sub> concentrations were determined by gas chromatography using a Hewlett Packard 5890 II gas chromatograph fitted with a 6 ft 5 Å molecular sieve column and a flame ionization detector following a headspace extraction in nitrogen [German *et al.*, 2010].

### 2.2.2. Total Organic Carbon Analysis

[10] Selected fluid samples were archived in 40 mL I-CHEM certified low-level total organic carbon (TOC) vials and frozen. TOC analyses were carried out at the University of California, Santa Barbara on a Shimadzu TOC-V series TOC analyzer as described in Carlson *et al.* [2010]. All samples were systematically standardized against low carbon water every 6–8 analyses, with deep Sargasso seawater (2600 m) and surface Sargasso seawater standards [Hansell and Carlson, 1998; Carlson *et al.*, 2004]. Daily standard waters were calibrated with DOC consensus waters standards. The analytical precision was  $\pm 0.9 \mu\text{M}$  ( $1\sigma$ ,  $n=3$ ) for deep reference water and  $\pm 0.7 \mu\text{M}$  ( $1\sigma$ ,  $n=3$ ) for surface reference water. Three to five replicate analyses were carried out on each sample to determine analytical precision.

### 2.3. Cell Counts

[11] Aliquots (18 mL) from selected CTD samples were preserved in formaldehyde (3.7% final concentration) in duplicate, and stored at 4°C for return to MBL (Woods Hole, MA) where cells were counted by

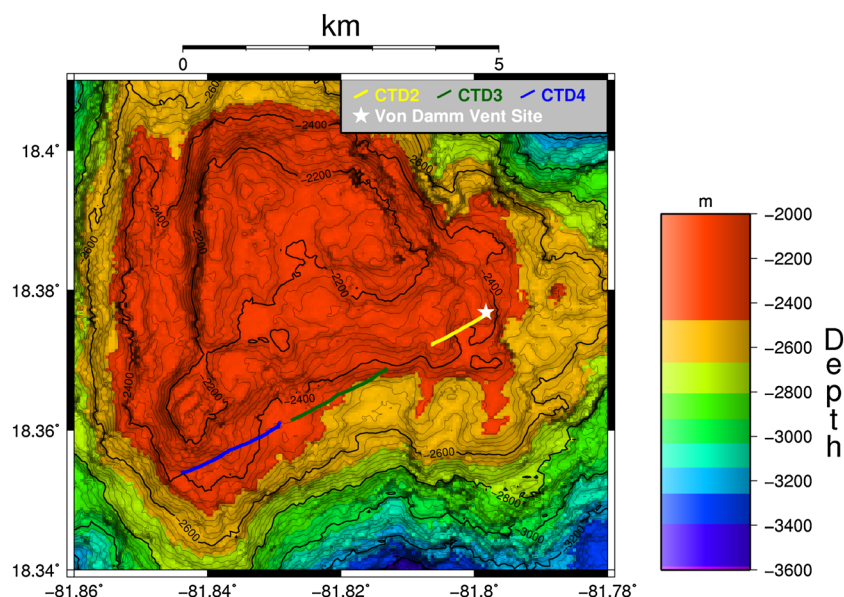


**Figure 1.** Map of the Von Damm Hydrothermal vent site (star), located on the eastern slope of Mt Dent. The location of the three Tow-Yo transects are shown (CTD 2 – yellow line, CTD 3 – green line, CTD 4 – blue line). A vertical cast (CTD 7) was also conducted, directly over the vent site (star).

epifluorescence microscopy with DAPI (4',6-diamidino-2-phenylindole, Sigma) [Porter and Feig, 1980].

### 3. Results

[12] Particles in the Von Damm hydrothermal plume, as detected using the in situ LSS, were observed up to ~1 km away from the vent-source (Figure 2A). However, even after in situ LSS anomalies fell to within background range ( $<0.02$  V), methane concentrations remained elevated at nonbuoyant plume height, reaching a maximum of 11.2 nM (Figure 3A, CTD 3). This compares to typical background methane concentrations of  $0.5 \pm 0.2$  nM ( $n=5$ ) (measured on a separate background CTD cast). These methane anomalies indicate further dispersal of hydrothermally influenced plume-water, devoid of suspended plume particles. The CTD cast carried out directly over the Von Damm mound (CTD 7) revealed elevated methane concentrations up to 43.7 nM that were accompanied by background levels of particles at nonbuoyant plume height. This observation is consistent with the fluids emanating from the central Von

Damm spire that are clear and devoid of suspended particulate matter [Connelly et al., 2012; German et al., 2012a, 2012b]. TOC concentrations ranged between 42.1 and 51.1  $\mu\text{M}$  and cell counts ranged between 0.5 and  $5.1 \times 10^4$  cells per mil indicating significant enrichments relative to background levels of  $43.2 \pm 0.7 \mu\text{M}$  ( $n=5$ ) and  $<1 \times 10^4$  cells/mL, respectively (Tables 1 and 2). The actual increase in total carbon that could be attributed to this cell increase from  $0.5 \times 10^4$  cells/mL to  $5.1 \times 10^4$  cells/mL can be calculated by assuming a cell has a weight of  $9.5 \times 10^{-13}$  g, of which 45% is carbon [Battley, 1998]. This would imply an overall increase in total organic carbon from cellular biomass of  $\sim 1.7 \mu\text{M}$ , representing a very small proportion of the TOC pool.

[13] Plume identification was made possible through temperature anomaly calculations [Baker, 1998], carried out as part of the immediate shore-based processing of data that followed each cast. These temperature anomalies result from the dilution of high-temperature end-member fluids ( $\leq 232^\circ\text{C}$ ) with surrounding seawater and allowed the Von Damm hydrothermal plume to be traced

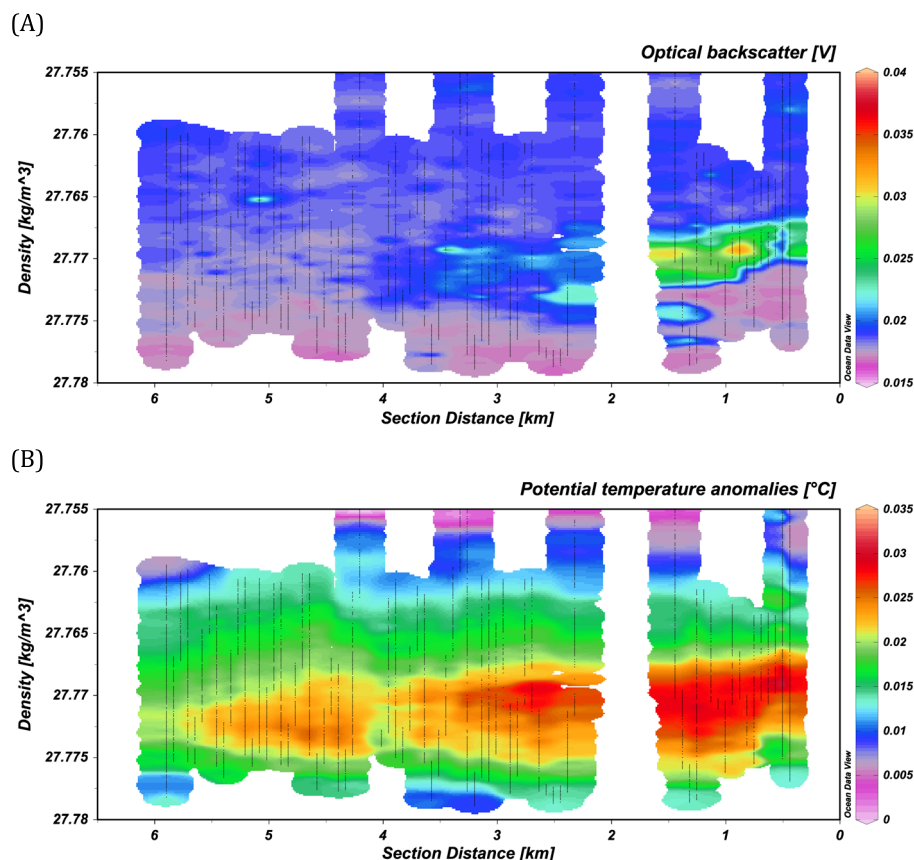


**Figure 2.** Combined Tow-Yo casts (CTD 2, 3, and 4) and vertical profile (CTD 7) from the Von Damm hydrothermal plume showing (A) optical backscatter anomalies and (B) potential temperature anomalies.



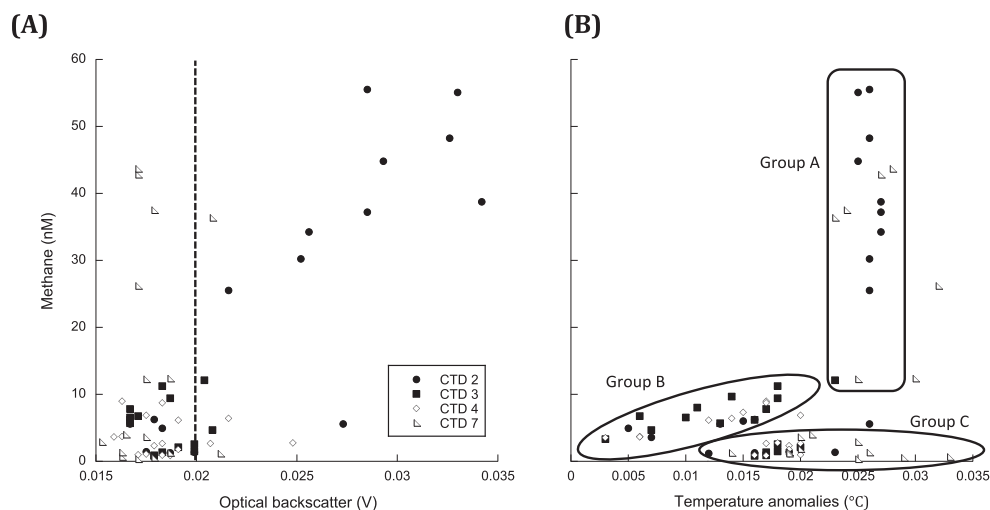


**Figure 3.** (A) Relationship between methane and optical backscatter in the hydrothermal plume. The dashed line at 0.02 V is the maximum optical backscatter value for background seawater in this region. (B) Relationship between methane and temperature anomalies in the hydrothermal plume. The selected groups of samples demonstrate similarities and are discussed in sections 4.1 and 4.2. For both figures, the four CTD deployments are represented by different symbols

**Table 1.** Data From the Three Tow-Yo Casts Where Samples Were Collected for Methane, TOC, and Cell Counts

	Depth (m)	OBS <sup>a</sup> (V)	CH <sub>4</sub> (nM)	TOC (μM)	σ	Cells/mL (× 10 <sup>4</sup> )	σ
CTD 2							
	2296	0.015	3.6	43.3	0.6	0.8	0.2
	2250	0.018	1.2	43.8	1.1	0.9	0.1
	2202	0.018	6.0			0.7	0.1
	2099	0.020	1.4			0.7	0.1
	2020	0.033	55.1	43.6	0.3	2.0	0.5
	2000	0.029	44.8	44.7	0.3	2.0	0.5
	1900	0.019	1.3	42.7	0.4	0.9	0.2
	2020	0.033	48.3	45.0	0.2	0.8	0.2
	2000	0.027	5.6	44.3	0.5	0.7	0.2
	2200	0.018	6.3	42.2	0.4	0.6	0.1
	2100	0.025	30.2	45.4	1.0	1.3	0.3
	2050	0.026	34.3			2.3	0.5
	2021	0.034	38.8			1.0	0.2
	1899	0.018	1.4			1.0	0.2
CTD 3							
	2399	0.017	3.3			0.6	0.2
	2296	0.019	8.0			2.9	0.4
	2200	0.018	9.7	47.3	0.1	2.8	0.6
	2100	0.018	0.8	45.4	1.0	1.9	0.5
	2000	0.019	9.4	46.1	0.5	3.1	0.8
	1900	0.018	1.4	47.7	0.9	1.3	0.3
CTD 4							
	2360	0.015	3.5			1.1	0.2
	2299	0.017				1.9	0.2
	2200	0.018	7.3	45.5	0.7	3.2	0.4
	2100	0.025	2.8			2.0	0.2
	2000	0.019	0.8	45.6	1.2	2.1	0.2
	1900	0.018	0.9	47.4	0.6	2.1	0.2
	2298	0.019	6.2	46.4	0.2		
	2198	0.016	9.0	46.8	1.0		
	2000	0.019	1.8	42.1	0.8		
	1900	0.018	1.1	42.9	1.4		

<sup>a</sup>OBS=Optical backscatter.

**Table 2.** Data From the Stationary CTD Cast Carried Out Above the Von Damm Vent Site, Including Samples Collected for Methane, TOC, and Cell Counts

	Depth (m)	OBS <sup>a</sup> (V)	CH <sub>4</sub> (nM)	TOC (μM)	σ	Cells/mL ( $\times 10^4$ )	σ
CTD 7							
	2324	0.019	1.4			0.9	0.1
	2300	0.018	1.3	51.1	1.3	1.1	0.1
	2300	0.021	1.1	45.2	1.1		
	2248	0.017	4.0	45.9	0.7	1.3	0.2
	2248	0.018	3.6	46.1	1.0		
	2203	0.018	37.5			0.7	0.2
	2203	0.021	36.4	44.5	1.4		
	2150	0.015	2.9			1.8	0.4
	2047	0.017	0.3			5.1	0.4
	1998	0.016	0.7	43.7	0.8	3.7	0.3
	1998	0.017	26.2	45.8	1.0	1.8	0.3
	1970	0.018	0.5	47.0	0.9	3.4	0.5
	1970	0.019	12.4			1.2	0.2
	2150	0.017	12.3	48.1	1.0	1.0	0.2
	2108	0.017	42.8			1.1	0.2
	2050	0.016	1.3			1.5	0.2
	1800	0.019	1.3	45.6	0.8	1.2	0.2

<sup>a</sup>OBS=Optical backscatter.

for ~5 km from its source during three separate Tow-Yo deployments (Figure 2B). Plume depth showed significant spatial and temporal variations, a feature that can be attributed to plume travel along isopycnal surfaces that change depth in response to tidal cycles and/or topography [Rudnicki *et al.*, 1994; Rudnicki and German, 2002; Bennett *et al.*, 2008]. By plotting the profiles against density, we can see that the plume sampled in all three Tow-Yo operations traveled along the same isopycnal surface consistent with dispersal away from a common vent-source. The aim of CTD 7 (vertical CTD cast, directly over the Von Damm mound) was to intercept the rising buoyant plume. However, it was very difficult to achieve this given the limited ship time available for the cast and the impact of deep ocean currents that impaired the precise positioning of the CTD-rosette at depth. Samples collected *below* nonbuoyant plume depth (Table 2, >2210 m) were both cooler and lower in methane concentrations than at nonbuoyant plume height (<4.0 nM). However, while the core of the buoyant plume would have been expected to be warmer than the nonbuoyant plume and more methane-rich, the samples we collected still exhibited elevated temperature anomalies compared to background and methane concentrations that were also greater than in background seawater. This combination of elevated temperatures and methane concentrations, coupled with the location of the CTD-rosette above the Von Damm mound suggest that while the CTD was not directly within the core of the buoyant plume at the time of sampling, it did still intercept the outer fringes of the rising, buoyant plume.

[14] In a previous study on the Mid-Cayman Rise, a plume was detected ~5 km SW from the Von Damm site that exhibited similar characteristics to the plumes reported here (albeit with a more pronounced Eh anomaly at lower maximum dissolved methane concentrations) [German *et al.*, 2010]. If there is another hydrothermal source in the vicinity of Von Damm, it is unlikely that it was sampled in this study. There were no deviations in the density of the dispersing plume, nor were there any unusual increases in temperature.

## 4. Discussion

### 4.1. Primary Productivity in the Near-Field Plume

[15] Chemical changes in dispersing hydrothermal plumes result from both dilution and chemical reactions between the source vent-fluids and the seawater that they mix with. Chemical reactions in the fluids may fuel chemosynthetic carbon fixation and have the potential to provide a source of labile organic carbon to the water column and underlying sediments [Roth and Dymond, 1989; Bennett *et al.*, 2011a, 2011b].

[16] To investigate potential primary productivity occurring in the Von Damm plume, we first consider changes in methane concentrations during plume dispersal. The abundance of methane in hydrothermal plumes may be influenced by microbial oxidation (methanotrophy), production (methanogenesis), and/or dilution [Anderson *et al.*, 1961].

Traditionally, methanogenesis was thought to occur only under fully anaerobic conditions; however, it has recently been detected in aerobic conditions as a result of methyl phosphonate decomposition in phosphate stressed waters [Karl *et al.*, 2008]. The maximum methane concentration measured in the Von Damm plume was 55 nM, occurring in seawater with temperature anomalies of 0.03°C (Figure 2A). This temperature anomaly results from the dilution of 232°C end-member fluid with the surrounding seawater at the seafloor (5.4°C) and suggests that the vent fluids have experienced a  $0.76 \times 10^4$ -fold dilution. Based on the measured dissolved methane concentration of 2.8 mM in end-member fluids venting at the summit of Von Damm (J. McDermott, pers. communication 2012), dilution of this magnitude should result in a plume concentration of 370 nM, substantially greater than the measured maximum of 55 nM. The nonconservative behavior of methane in the hydrothermal plume provides compelling evidence for consumption via active microbial methane oxidation [De Angelis *et al.*, 1993; Cowen *et al.*, 2002; Gamo *et al.*, 2003].

[17] Continued dilution and consumption of methane in the dispersing hydrothermal plume can be evaluated by plotting all the methane data relative to temperature anomalies (Figure 3B). While no single relationship can describe the entire data set, there does appear to be relationships in select groups of samples. One group of samples, at a temperature anomaly of  $0.025 \pm 0.005^\circ\text{C}$ , appear to have experienced the same dilution, but exhibit widely varying, elevated, methane concentrations (Group A). This suggests that in these relatively “fresh” plume samples methanotrophy is active. During chemoautotrophic carbon fixation, there should be an increase in cellular biomass and extracellular carbon release into the TOC pool and this may explain the elevated TOC concentrations in the Von Damm plume (42.1 and 51.1 μM (background =  $43.2 \pm 0.7 \mu\text{M}$  ( $n=5$ )). However, it has previously been reported that variations in organic carbon concentrations in plumes may also result from entrainment of organic carbon from areas of high productivity on the seafloor surrounding a vent site [Bennett *et al.*, 2011b] or even from the end-member fluids themselves (in the case of ultramafic-hosted systems) [Konn *et al.*, 2009]. Neither of these two carbon sources are likely to be responsible for the elevated TOC concentrations present in our samples, because the temperature anomalies in the plume infer that a  $0.76 \times 10^4$ -fold dilution has occurred during buoyant plume rise (see above).

Consequently, any elevated concentrations of TOC in the end-member fluids or from entrainment of TOC-enriched diffuse flow close to the seafloor, should have been diluted out by surrounding seawater during buoyant plume rise [Bennett *et al.*, 2011b]. Any enrichment in TOC in our plume samples must therefore be a result of in situ productivity. By plotting TOC versus methane concentrations (Figure 4A), we can see that for samples that have experienced the same dilution (same temperature anomalies, Group A), TOC increases with decreasing methane concentrations. Not all the methane samples were analyzed for TOC (hence, there are fewer data points in this plot compared to Figure 3B) but nevertheless, the inverse correlation between TOC and methane concentrations argues strongly for biological productivity occurring at the same time as microbially mediated methane oxidation in this region of the dispersing Von Damm plume.

[18] It is important to note, however, that methane oxidation, itself, cannot be responsible for the coincident increase in TOC, because there is only enough energy available from the oxidation of methane to produce 1–2% of the 5 μM enrichment in total organic carbon observed. If oxidation of 1 mol of methane results in a Gibbs free energy change of –192 kcal (–803 kJ) as estimated by McCollom [2000], the oxidation of 55 nM of methane (the maximum values reported here from anywhere within the nonbuoyant Von Damm plume) could yield no more than  $\sim 10^{-2}$  cal/L (44 J per L). In comparison, the energy required to fix 1 μM of a simple glucose molecule is  $6.9 \times 10^{-1}$  cal/L (2887 J per L) [Battley, 1998]. This suggests that other autotrophic carbon fixation pathways must occur in parallel with the oxidation of methane to account for the elevated TOC concentrations observed. As this is an ultramafic influenced hydrothermal system, elevated hydrogen concentrations will be expected and will provide a large amount of energy for carbon fixation. Elevated sulfur concentrations known to be present in the Von Damm plume [Connelly *et al.*, 2012] suggest that sulfur oxidation could be another important energy pathway. Sulfide oxidation and ammonium oxidation may also provide sources of energy available within the Von Damm plume [McCollom, 2000; Baker *et al.*, 2012]. The 2009 hydrothermal plume detected 5 km SW of the Von Damm site was rich in the sulfur oxidizing microbial groups *Epsilonproteobacteria Sulfurimonas* and *Gammaproteobacteria SUP05* [German *et al.*, 2010], both of which have been found to be prevalent in plumes from other hydrothermal systems [Sunamura *et al.*, 2004; Nakagawa

*et al.*, 2005; Dick and Tebo, 2010; Baker *et al.*, 2012; Lesniewski *et al.*, 2012] and, indeed, are ubiquitous in the mesopelagic deep ocean [Swan *et al.*, 2011]. Such organisms may be responsible for the elevated TOC concentrations in the plume sampled during this study.

#### 4.2. Cycling in the Dispersing Von Damm Plume

[19] Two further distinct groups of samples exist in the Von Damm plume. Both sample groups span a range of potential temperature anomalies (Figure 3B) indicating dilution with ambient seawater to varying extents. Of these two, the samples most concentrated in methane (Group B) appear to decrease in methane concentration with increasing plume dilution (decreasing potential temperature anomalies; Figure 3B). The same is true for their TOC concentration, which also show a linear decrease with decreasing methane concentration (Figure 4A). This suggests that dilution is driving the changes in methane concentrations in this portion of the Von Damm plume. Interestingly, using the linear relationship between TOC and methane defined by these Group B samples we can predict that, at background methane concentrations (0.5 nM), the TOC concentration should be 41  $\mu$ M, which provides reassuringly close convergence with the concentration expected for deep ocean Caribbean waters [Carlson *et al.*, 2010]. The majority of the samples in Group B were

collected from CTD casts 3 and 4 and, hence, represent the more distal portions of the Von Damm nonbuoyant plume. The relationship between TOC and methane in these far field samples therefore reflects dilution and suggests primary productivity is inhibited. However, the ranges of observed cell concentrations are significantly greater in the distal plume relative to the near-field (Group A) nonbuoyant plume samples (Figure 4B) and suggests another possibility, that *if* there is any primary productivity occurring in the distal plume, consumption by mixotrophic and/or heterotrophic microorganisms must also be occurring.

[20] The third and final group of samples collected in this study (Group C) exhibit uniformly low methane concentrations ( $\leq 4.0$  nM), but span the widest range of potential temperature anomalies (0.012–0.033°C; Figure 3B). These samples come from all four CTD casts and, at 42.1–51.1  $\mu$ M, their TOC and cell concentrations span the widest range of values of all three groups (Figures 4A and 4B). These samples come from the fringes of the nonbuoyant and buoyant Von Damm plume, along its entire dispersal trajectory. In previous studies, both positively and negatively buoyant lipid-rich particles have been detected emanating from hydrothermal plumes, and high concentrations of zooplankton have been documented within the 100 m layer above hydrothermal plumes at Endeavour segment, Juan de Fuca Ridge [Cowen *et al.*, 2001; Wakeham *et al.*, 2001]. Organic-rich material on the edges of the plume

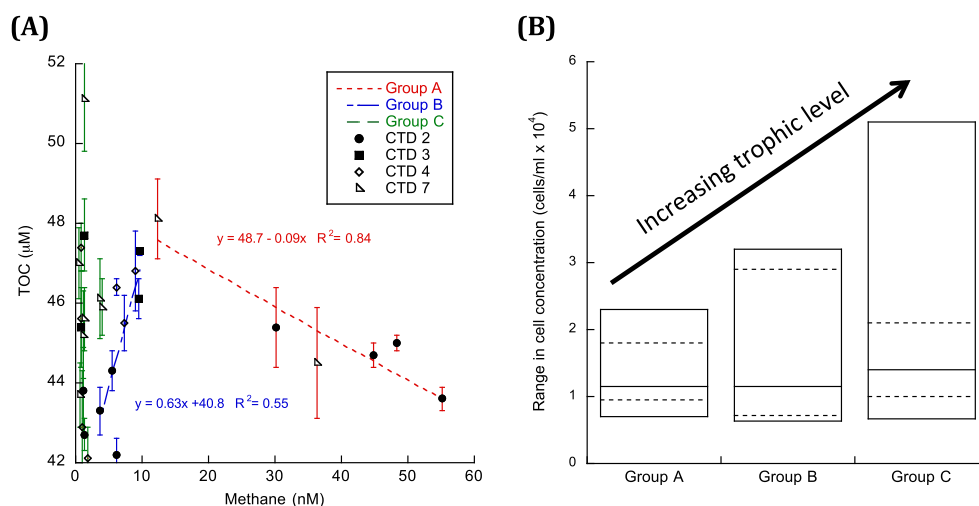


**Figure 4.** (A) Relationship between TOC and methane for individual groups of samples identified in Figure 3b. Error bars for TOC are as in Tables 1 and 2. Not all the methane samples were analyzed for TOC and therefore there are fewer data points in this plot compared to Figure 3B. (B) A percentile graph of cell counts for individual groups of samples characterized in Figure 3B, demonstrating the range of cell concentrations observed. The bottom and top of each box represent 5% and 95% of the data, while the lower and upper dashed lines represent 25% and 75% of the data. The solid middle line represents the median.



may be the result of vent larvae, transparent exopolymer particles or organic material (polysaccharides, proteins) hypothesized to be produced by plume microbes as a result of chemosynthesis [Mullineaux *et al.*, 1995; Shackelford and Cowen, 2006; Breier *et al.*, 2012]. We postulate, therefore, that the data from Group C may be indicative of a community of heterotrophic microorganisms fuelled by plume-supplied nutrients. Microbial consumer studies in the hydrothermal plume have previously concentrated on the zooplankton living off upper plume edges [Cowen *et al.*, 2001; Burd *et al.*, 2002; Vinogradov *et al.*, 2003]. In our study, the greater cell numbers were all within a similar size range ( $\sim 1 \times 1 \mu\text{m}$ ), whereas zooplankton are much larger ( $>100 \mu\text{m}$ ). Consequently, we hypothesize that consumers in the Von Damm plume are smaller microbial heterotrophs and mixotrophs (e.g., bacteria, viruses and small eukaryotic protists). Examples of such organisms have been detected previously in other hydrothermal vent systems [Atkins *et al.*, 2000; Ortmann and Suttle, 2005; Kaye *et al.*, 2011; Sylvan *et al.*, 2012].

[21] Taken together, our data allow three distinct regions within the Von Damm hydrothermal plume to be identified:

- (1) The near-field plume, where chemoautotrophic primary production results in increased organic carbon production

- (2) The more distal nonbuoyant plume where dilution dominates and any, if present at all, in situ carbon production is matched by carbon consumption
- (3) The fringes of the buoyant and nonbuoyant plume, where heterotrophy results in increased cellular biomass and TOC.

[22] In sequence, these three regions allow a microbial food web to be hypothesized, with relative plume locations, from primary productivity to primary and secondary consumers (Figure 5). This is most clearly reflected in the increasing range of cell concentrations observed from Groups A to C (Figure 4B). The role of chemoautotrophy as a food source to macroinvertebrates at deep-sea hydrothermal vents and cold seeps is well recognized, but limited to the immediate locality of the venting fluids. In comparison, the dispersing hydrothermal plume also hosts a chemoautotrophic community and can provide an important carbon and energy source to higher trophic levels in the microbial food web. Energy sources are both entrained and produced in situ, providing the energy to both the base of the food web and the microbial heterotrophs and mixotrophs at increasing trophic levels (Figure 5).

[23] In our study, elevated concentrations of organic carbon have been detected beyond the near vent environment ( $\sim 5 \text{ km}$ ) and may continue to host a microbial food web even farther afield (up to

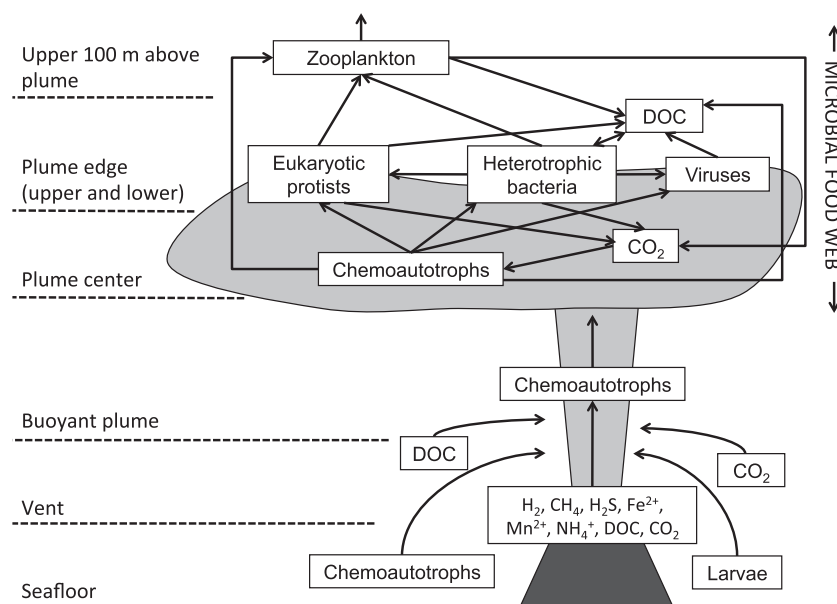


**Figure 5.** Schematic of a deep-sea hydrothermal plume with the proposed microbial food web and relative trophic positions within the plume. The lower half of the schematic represents the entrainment of energy sources from the vent fluids and the surrounding vent field, which fuel the microbial food web in the plume. DOC = Dissolved Organic Carbon.

25 km [Burd *et al.*, 2002]). Chemoautotrophically fueled microbial food webs are recognized elsewhere in the ocean, such as at oxygen minimum zones and at the redox transition zone of an anoxic basin [Taylor *et al.*, 2001; Podlaska *et al.*, 2012], and methanotrophy has been identified as an important food source to higher trophic levels [Deines *et al.*, 2007]. We recommend that the complete microbial food web should be considered in all future hydrothermal plume studies that seek to evaluate the potential sources and sinks of carbon from hydrothermal venting to the deep ocean.

## 5. Summary

[24] By using potential temperature anomalies as a conservative tracer, we have been able to trace a particle-deplete hydrothermal plume 5 km from its source and detect elevated concentrations of total organic carbon reaching a maximum of 51.1  $\mu\text{M}$ . We have identified three distinct regions within the dispersing Von Damm hydrothermal plume that appear to host primary producers and primary and secondary consumers, respectively. This has enabled us to hypothesize the presence of a microbial food web within the dispersing hydrothermal plume that should provide an important conceptual framework for any future studies that seek to evaluate sources and sinks of carbon from hydrothermal venting to the deep ocean.

## Acknowledgments

[25] We thank the Commanding Officer and Crew of the NOAA Ship Okeanos Explorer cruise EX11-04 Mid-Cayman Rise Expedition and R/V *Atlantis* AT18-16 together with the Okeanos Explorer Mission team and ROV Jason team without which this research would not have been possible. The research reported in this paper was supported by ship time and support provided by NOAA's Office of Ocean Exploration and Research and the Office of Marine and Aviation Operations and NSF's Division of Ocean Sciences (Grant OCE-1061863) and by further shore-based research from both the National Science Foundation (NSF OCE-1061863) and NASA's ASTEP Program (Grant # NNX09AB75G). The contributions of SB and MC were carried out at the Jet Propulsion Laboratory (JPL), California Institute of Technology, under contract with the National Aeronautics and Space Administration (NASA), with support from the NASA ASTEP Program.

## References

Anderson, R. B., K. C. Stein, J. J. Feenan, and L. J. E. Hofer (1961), Catalytic oxidation of methane, *Ind. Eng. Chem.*, 53(10), 809–812.

Atkins, M. S., A. P. Teske, and O. R. Anderson (2000), A survey of flagellate diversity at four deep-sea hydrothermal

vents in the Eastern Pacific Ocean using structural and molecular approaches, *J. Eukaryot. Microbiol.*, 47(4), 400–411.

Baker, B. J., R. A. Lesniewski, and G. J. Dick (2012), Genome-enabled transcriptomics reveals archaeal populations that drive nitrification in a deep-sea hydrothermal plume, *ISME J.*, 6, 2269–2279.

Baker, E. T. (1998), Patterns of event and chronic hydrothermal venting following a magmatic intrusion: new perspectives from the 1996 Gorda Ridge eruption, *Deep. Sea Res. Topic. Stud. Oceanogr.*, 45(12), 2599–2618.

Battley, E. H. (1998), The development of direct and indirect methods for the study of the thermodynamics of microbial growth, *Thermochim. Acta*, 309(1–2), 17–37.

Bennett, S. A., R. L. Hansman, A. L. Sessions, K. Nakamura, and K. J. Edwards (2011a), Tracing iron-fueled microbial carbon production within the hydrothermal plume at the Loihi seamount, *Geochim. Cosmochim. Acta*, 75(19), 5526–5539.

Bennett, S. A., E. P. Achterberg, D. P. Connelly, P. J. Statham, G. R. Fones, and C. R. German (2008), The distribution and stabilisation of dissolved Fe in deep-sea hydrothermal plumes, *Earth Planet. Sci. Lett.*, 270, 157–167.

Bennett, S. A., P. J. Statham, D. R. H. Green, N. Le Bris, J. M. McDermott, F. Prado, O. J. Rouxel, K. Von Damm, and C. R. German (2011b), Dissolved and particulate organic carbon in hydrothermal plumes from the East Pacific Rise, 9 degrees 50 ' N, *Deep. Sea Res. Oceanogr. Res. Paper.*, 58(9), 922–931.

Breier, J. A., B. M. Toner, S. C. Fakra, M. A. Marcus, S. N. White, A. M. Thurnherr, and C. R. German (2012), Sulfur, sulfides, oxides and organic matter aggregated in submarine hydrothermal plumes at 9 degrees 50 ' N East Pacific Rise, *Geochim. Cosmochim. Acta*, 88, 216–236.

Burd, B. J., R. E. Thomson, and S. E. Calvert (2002), Isotopic composition of hydrothermal epiplume zooplankton: evidence of enhanced carbon recycling in the water column, *Deep. Sea Res. Oceanogr. Res. Paper.*, 49(10), 1877–1900.

Carlson, C. A., S. J. Giovannoni, D. A. Hansell, S. J. Goldberg, R. Parsons, and K. Vergin (2004), Interactions among dissolved organic carbon, microbial processes, and community structure in the mesopelagic zone of the northwestern Sargasso Sea, *Limnol. Oceanogr.*, 49(4), 1073–1083.

Carlson, C. A., D. A. Hansell, N. B. Nelson, D. A. Siegel, W. M. Smethie, S. Khatiwala, M. M. Meyers, and E. Halewood (2010), Dissolved organic carbon export and subsequent remineralization in the mesopelagic and bathypelagic realms of the North Atlantic basin, *Deep. Sea Res. Topic. Stud. Oceanogr.*, 57(16), 1433–1445.

Charlou, J. L., Y. Fouquet, H. Bougault, J. P. Donval, J. Etoubleau, P. Jean-Baptiste, A. Dapigny, P. Appriou, and P. A. Rona (1998), Intense CH<sub>4</sub> plumes generated by serpentinization of ultramafic rocks at the intersection of the 15 degrees 20 ' N fracture zone and the Mid-Atlantic Ridge, *Geochim. Cosmochim. Acta*, 62(13), 2323–2333.

Connelly, D. P., et al. (2012), Hydrothermal vent fields and chemocynthetic biota on the world's deepest seafloor spreading centre, *Nature Communications*.

Corliss, J. B., J. Dymond, L. I. Gordon, J. M. Edmond, R. P. V. Herzen, R. D. Ballard, K. Green, D. Williams, A. Bainbridge, K. Crane, and T. H. Vanandel (1979), Submarine Thermal Springs on the Galapagos Rift, *Science*, 203 (4385), 1073–1083.

Cowen, J. P., X. Y. Wen, and B. N. Popp (2002), Methane in aging hydrothermal plumes, *Geochim. Cosmochim. Acta*, 66(20), 3563–3571.

Cowen, J. P., M. A. Bertram, S. G. Wakeham, R. E. Thomson, J. W. Lavelle, E. T. Baker, and R. A. Feely (2001),

- Ascending and descending particle flux from hydrothermal plumes at Endeavour Segment, Juan de Fuca Ridge, *Deep. Sea Res. Oceanogr. Res. Paper.*, 48(4), 1093–1120.
- De Angelis, M. A., M. D. Lilley, E. J. Olson, and J. A. Baross (1993), Methane oxidation in the deep-sea hydrothermal plumes of the Endeavor Segment of the Juan de Fuca Ridge, *Deep. Sea Res. Oceanogr. Res. Paper.*, 40(6), 1169–1186.
- Deines, P., P. L. E. Bodelier, and G. Eller (2007), Methane-derived carbon flows through methane-oxidizing bacteria to higher trophic levels in aquatic systems, *Environ. Microbiol.*, 9(5), 1126–1134.
- Dick, G. J., and B. M. Tebo (2010), Microbial diversity and biogeochemistry of the Guaymas Basin deep-sea hydrothermal plume, *Environ. Microbiol.*, 12(5), 1334–1347.
- Gamo, T., U. Tsunogai, S. Ichibayashi, A. Hirota, and K. H. Shipboard Sci Parties (2003), “Microbial plumes” as inferred from the increase of stable carbon isotope composition of methane originated from submarine hydrothermal activity, *Geochim. Cosmochim. Acta*, 67(18), A115–A115.
- German, C. R., and W. E. Seyfried Jr (In press), Hydrothermal Processes, in *Treatise of Geochemistry: The oceans and marine geochemistry*, edited, 2nd Edition, Elsevier-Pergamon, Oxford, Oxford.
- German, C. R., et al. (2012a), Exploration of the Mid-Cayman Rise, *Oceanography*, 25(1 - Supplement), 52–53.
- German, C. R., et al. (2010), Diverse styles of submarine venting on the ultraslow spreading Mid-Cayman Rise, *Proc. Natl. Acad. Sci. U.S.A.*, 107(32), 14020–14025.
- German, C. R., et al. (2012b), RV Atlantis & ROV Jason AT18-16 (Oases 2012) Cruise Report, 75pp.
- Hansell, D. A., and C. A. Carlson (1998), Deep-ocean gradients in the concentration of dissolved organic carbon, *Nature*, 395(6699), 263–266.
- Hayman, N. W., N. R. Grindlay, M. R. Perfit, P. Mann, S. Leroy, and B. M. de Lepinay (2011), Oceanic core complex development at the ultraslow spreading Mid-Cayman Spreading Center, *Geochem. Geophys. Geosyst.*, 12.
- Karl, D. M., L. Beversdorf, K. M. Bjorkman, M. J. Church, A. Martinez, and E. F. DeLong (2008), Aerobic production of methane in the sea, *Nat. Geosci.*, 1(7), 473–478.
- Kaye, J. Z., J. B. Sylvan, K. J. Edwards, and J. A. Baross (2011), Halomonas and Marinobacter ecotypes from hydrothermal vent, seafloor and deep-sea environments, *FEMS Microbiol. Ecol.*, 75(1), 123–133.
- Konn, C., J. L. Charlou, J. P. Donval, N. G. Holm, F. Dehairs, and S. Bouillon (2009), Hydrocarbons and oxidized organic compounds in hydrothermal fluids from Rainbow and Lost City ultramafic-hosted vents, *Chem. Geol.*, 258(3–4), 299–314.
- Lesniewski, R., S. Jain, K. Anantharaman, P. Schloss, and G. J. Dick (2012), The metatranscriptome of a deep-sea hydrothermal plume is dominated by water column methanotrophs and chemolithotrophs, *ISME J.*, 6, 2257–2268, doi:10.1038/ismej.2012.63.
- Lupton, J. E., J. R. Delaney, H. P. Johnson, and M. K. Tivey (1985), Entrainment and Vertical Transport of Deep-Ocean Water by Buoyant Hydrothermal Plumes, *Nature*, 316(6029), 621–623.
- McCollom, T. M. (2000), Geochemical constraints on primary productivity in submarine hydrothermal vent plumes, *Deep. Sea Res. Oceanogr. Res. Paper.*, 47(1), 85–101.
- Mullineaux, L. S., P. H. Wiebe, and E. T. Baker (1995), Larvae of benthic invertebrates in hydrothermal vent plumes over Juan-de-Fuca Ridge, *Mar. Biol.*, 122(4), 585–596.
- Nakagawa, S., K. Takai, F. Inagaki, H. Hirayama, T. Nunoura, K. Horikoshi, and Y. Sako (2005), Distribution, phylogenetic diversity and physiological characteristics of epsilon-Proteobacteria in a deep-sea hydrothermal field, *Environ. Microbiol.*, 7(10), 1619–1632.
- Ortmann, A. C., and C. A. Suttle (2005), High abundances of viruses in a deep-sea hydrothermal vent system indicates viral mediated microbial mortality, *Deep. Sea Res. Oceanogr. Res. Paper.*, 52(8), 1515–1527.
- Podlaska, A., S. G. Wakeham, K. A. Fanning, and G. T. Taylor (2012), Microbial community structure and productivity in the oxygen minimum zone of the eastern tropical North Pacific, *Deep. Sea Res. Oceanogr. Res. Paper.*, 66, 77–89.
- Porter, K. G., and Y. S. Feig (1980), The use of DAPI for identifying and counting aquatic microflora, *Limnol. Oceanogr.*, 25(5), 943–948.
- Roth, S. E., and J. Dymond (1989), Transport and settling of organic material in a deep-sea hydrothermal plume: evidence from particle flux measurements, *Deep. Sea Res. Oceanogr. Res. Paper.*, 36(8), 1237–1254.
- Rudnicki, M. D., and C. R. German (2002), Temporal variability of the hydrothermal plume above the Kairei vent field, 25 degrees S, Central Indian Ridge, *Geochem. Geophys. Geosyst.*, 3, 1010 Feb 1019 2002.
- Rudnicki, M. D., R. H. James, and H. Elderfield (1994), Near-Field Variability of the Tag Non-buoyant Plume, 26-Degrees-N, Mid-Atlantic Ridge, *Earth Planet. Sci. Lett.*, 127(1–4), 1–10.
- Shackelford, R., and J. P. Cowen (2006), Transparent exopolymer particles (TEP) as a component of hydrothermal plume particle dynamics, *Deep. Sea Res. Oceanogr. Res. Paper.*, 53(10), 1677–1694.
- Shock, E. L. (1990), Geochemical constraints on the origin of organic-compounds in hydrothermal systems, *Orig. Life Evol. Biosph.* 20(3–4), 331–367.
- Shock, E. L., and M. D. Schulte (1998), Organic synthesis during fluid mixing in hydrothermal systems, *J. Geophys. Res. - Planets*, 103(E12), 28513–28527.
- Sunamura, M., Y. Higashi, C. Miyako, J. Ishibashi, and A. Maruyama (2004), Two bacteria phylotypes are predominant in the Suiyo Seamount hydrothermal plume, *Appl. Environ. Microbiol.*, 70(2), 1190–1198.
- Swan, B. K., et al. (2011), Potential for Chemolithoautotrophy Among Ubiquitous Bacteria Lineages in the Dark Ocean, *Science*, 333(6047), 1296–1300.
- Sylvan, J. B., B. C. Pyenson, O. Rouxel, C. R. German, and K. J. Edwards (2012), Time-series analysis of two hydrothermal plumes at 9 degrees 50'N East Pacific Rise reveals distinct, heterogeneous bacterial populations, *Geobiology*, 10(2), 178–192.
- Taylor, G. T., M. Iabichella, T. Y. Ho, M. I. Scranton, R. C. Thunell, F. Muller-Karger, and R. Varela (2001), Chemoautotrophy in the redox transition zone of the Cariaco Basin: A significant midwater source of organic carbon production, *Limnol. Oceanogr.*, 46(1), 148–163.
- Van Dover, C. L. (2000), *The Ecology of Deep-Sea Hydrothermal Vents*, Princeton University Press, Princeton.
- Vinogradov, G. M., A. L. Vereshchaka, and D. L. Aleinik (2003), Zooplankton distribution over hydrothermal fields of the Mid-Atlantic Ridge, *Oceanology*, 43(5), 656–669.
- Wakeham, S. G., J. P. Cowen, B. J. Burd, and R. E. Thomson (2001), Lipid-rich ascending particles from the hydrothermal plume at Endeavour Segment, Juan de Fuca Ridge, *Geochim. Cosmochim. Acta*, 65(6), 923–939.
- Winn, C. D., D. M. Karl, and G. J. Massoth (1986), Microorganisms in Deep-Sea Hydrothermal Plumes, *Nature*, 320 (6064), 744–746.